



# Atom Lithography

Vasant Natarajan

**Abstract** | We review the two kinds of forces that near-resonant light exerts on atoms—the spontaneous force that is used for laser cooling, and the stimulated force that is used for coherent manipulation of atoms. We will discuss an experiment where laser cooling is used to collimate an atomic beam of sodium atoms, and the stimulated force within one period of a one-dimensional standing wave is used as a lens to focus the atoms to a narrow line about 20 nm wide. This kind of atom lithography is an example of the general field of atom optics in which light is used to manipulate atoms.

This article will serve as a prelude to the rest of the articles in this special issue on cold atoms because we discuss both kinds of forces of near-resonant light on atoms—the **spontaneous** or scattering force which is used for laser cooling;<sup>\*</sup> and the **dipole** or stimulated force which is a conservative force and hence can be derived from a potential, in an optical lattice for example. In the experiment described here, transverse laser cooling will be first used to collimate an atomic beam of sodium atoms, then the dipole force within a period of a standing wave (SW) of light will be used as a lens to focus the atoms on to a silicon substrate—this is atom *nano*-lithography since the deposited line is only 20 nm wide. Most of the results presented here are published in Ref. 1.

## 1 Spontaneous Force

This force arises because each photon carries a momentum of  $\hbar k$ , where  $k = 2\pi/\lambda$  is the wavevector. By momentum conservation, this quantum of momentum gets transferred to the atom each time it absorbs or emits a photon. The momentum transfer is in the direction of the laser beam for absorption, and in a random direction for emission. Thus, after  $n$  absorption-emission cycles, the average momentum transferred is  $n\hbar k$  in the direction of the laser beam, because the average for the emission cycles is zero. The random nature of the emission cycles is important for laser cooling because the entropy of the atomic system has to be decreased to achieve cooling, and this decrease

in entropy has to be compensated by an increase in entropy somewhere, the somewhere being the photon field in this case.

To understand laser cooling, let us first consider it in one dimension (1D). Imagine a simple case where the atom has just two levels  $|g\rangle$  and  $|e\rangle$  with a transition frequency  $\omega_0$ , as shown in Fig. 1. Now consider that the atom is bombarded with identical laser beams from the left and the right sides, both of which are detuned below resonance. If the atom is stationary, Fig. 1(a) shows that the scattering rate (and hence the force) of the two laser beams is equal. However, if an atom is moving to the right with a small velocity  $v$ , then the laser beam on the right is Doppler-shifted closer to resonance compared to the laser beam on the left. As a consequence, the atom scatters more photons from the right beam and feels a force to the left. The opposite happens for an atom moving to the left—it Doppler shifts the left beam closer to resonance, scatters more photons from that beam, and thus feels a force to the right. Therefore the force always opposes the motion, and behaves like a frictional force that results in cooling. Another way to think about it is that the detuning below resonance means that the photon has less energy than is required for the atomic transition, it makes up for this shortfall using the kinetic energy of the atom, thus reducing the kinetic energy and cooling the atom in the process. Such a configuration of laser beams has been colorfully called “Optical Molasses” to highlight the fact that the atom feels a viscous drag on its motion. And the 1D model considered above can be readily extended to 3D by having three sets of counter-propagating beams in the three orthogonal directions.

<sup>\*</sup>See special issue on *Laser Cooling and Trapping of Atoms*, edited by Steven Chu and Carl Wieman [J. Opt. Soc. Am. B 6, 2020–2078 (1989)].

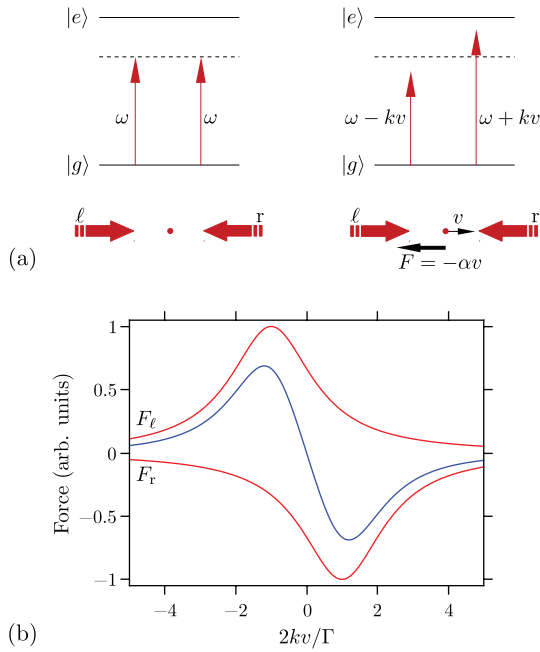


**Figure 1:** Laser cooling of atoms in 1D using optical molasses. The two laser beams are equally detuned below resonance. (a) The two forces are equal when the atom is stationary; but become unequal when the atom is moving with a velocity  $v$ , because one beam is Doppler-shifted closer to resonance. (b) Forces due to the left beam (red), right beam (red), and their sum (blue), as a function of velocity, for the configuration shown in (a). The detuning is chosen to be  $\Delta = -2kv/\Gamma$ .

The above analysis can be quantified by considering the force due to each laser beam, which is just the photon momentum times the scattering rate. For an atom moving with a velocity  $v$ , the force due to the left beam is

$$F_{\ell}(v) = +\hbar k \frac{\Gamma}{2} \frac{I/I_s}{1 + I/I_s + [2(\Delta - kv)/\Gamma]^2} \quad (1)$$

where  $\Gamma$  is the linewidth of the transition;  $I$  is the intensity of the laser beam, the scale for which is set by the saturation intensity  $I_s$  defined as the intensity at which the transition gets power broadened by a factor of  $\sqrt{2}$ ; and  $\Delta = \omega - \omega_0$  is the detuning from resonance in the lab frame (with an additional  $-kv$  term in the atom's frame). The detuning is normally measured in frequency units (Hz) as  $\delta$ , which is  $\Delta/2\pi$ .

We can show similarly that the force from the right beam is

$$F_r(v) = -\hbar k \frac{\Gamma}{2} \frac{I/I_s}{1 + I/I_s + [2(\Delta + kv)/\Gamma]^2} \quad (2)$$

The total force on the atom is the sum of these two forces, which, in the limit of low intensity and small atomic velocity, can be approximated as

$$F = F_{\ell} + F_r \approx 4\hbar k \frac{I}{I_s} \frac{kv(2\Delta/\Gamma)}{[1 + (2\Delta/\Gamma)^2]^2} \quad (3)$$

Thus the total force is linear in  $\Delta$  and  $v$ , and is a frictional force ( $\sim -v$ ) when the detuning is negative.

The two forces as a function of velocity along with their sum are shown in Fig. 1(b). Analysis of the above equation shows that the lowest temperature—called the *Doppler cooling limit*—is reached when the detuning  $\Delta = -\Gamma/2$ , and the temperature reached is  $k_B T_{\min} = \hbar\Gamma/2$ . This is the detuning chosen for the curves shown in the figure. The total force is clearly linear with a negative slope for small  $v$ . The velocity for which each force reaches a maximum for this detuning is  $v_{\text{cap}} = \Gamma/(2k)$ , which is called the capture velocity of the molasses—the atomic velocity has to be of this order for it to be cooled effectively. In order to give some numbers, for sodium atoms cooled on the  $D_2$  line used in the experiment,  $T_{\min} = 240 \mu\text{K}$  and  $v_{\text{cap}} = 2.95 \text{ m/s}$ .

Though this is a low temperature, one would think that the recoil velocity of the atom after emitting a photon should be the limit for laser cooling, i.e. the lowest temperature is reached when  $v_{\text{rms}} = \hbar k/m_a$  for an atom of mass  $m_a$ . This temperature is one to two orders of magnitude lower than the Doppler cooling limit considered above. Careful experiments in the 1980's showed that such temperatures could indeed be reached with what is called “polarization-gradient cooling”. The mechanism is more complicated, and requires understanding of light shifts in atoms for different polarizations, larger detunings, and careful nulling of magnetic fields. The rather involved theory is reviewed extensively in Refs. 2 and 3, but experimentally it is easy to implement. In the experiments discussed here, both Doppler cooling and polarization-gradient cooling have been used, and we will see the difference between the two.

## 2 Dipole Force

This force is a coherent force that arises because the atom is driven coherently between the two levels by the laser. The incoherent nature of spontaneous emission from  $|e\rangle$  is ignored, which becomes an increasingly better approximation as the detuning is increased. The easiest way to understand the force is that, as the name implies, it is due to the induced dipole moment in the atom by the light. Since the induced dipole moment is proportional

to the amplitude of the incident electric field  $E_0$ , the energy is proportional to  $E_0^2$  (with a factor of 2 to account for the fact that it is induced and not permanent, the same factor of 2 appears in the familiar energy stored in a capacitor). Thus the energy is proportional to the light intensity and can cause a force if the intensity is inhomogeneous. One way to create such intensity variation is by having a 1D standing wave using two identical counter-propagating light beams—a 1D optical lattice.

In order to get a quantitative measure of the force, it is useful to define the saturation parameter  $p$  given by

$$p = \frac{I}{I_s} \frac{1}{1 + 4\Delta^2/\Gamma^2} \quad (4)$$

because then the force can be derived from the potential<sup>4</sup>

$$U = \frac{\hbar\Delta}{2} \sqrt{1 + 2p} \quad (5)$$

This is the AC Stark shift of the levels by the laser, also called the dressed-state potential. For large detuning  $|\Delta|/\Gamma \ll 1$  which implies  $p \ll 1$ , so that it can be approximated as

$$p \approx \frac{I}{I_s} \frac{\Gamma^2}{4\Delta^2} \quad (6)$$

Hence the potential can be expanded as

$$U \approx \frac{\hbar\Delta}{2} \left[ 1 + \frac{I}{I_s} \frac{\Gamma^2}{4\Delta^2} \right] = \frac{\hbar\Delta}{2} + \frac{\hbar\Gamma^2}{8\Delta} \frac{I}{I_s} \quad (7)$$

Ignoring the constant term  $\hbar\Delta/2$ , the above expression shows that the potential varies as  $I/\Delta$ , and therefore although the potential becomes more coherent with increasing detuning (the effect of  $|e\rangle$  becomes smaller) it comes at the price of requiring more intensity to get the same potential depth.

With increasing detuning, the potential also becomes more harmonic and deeper. This should be clear by looking at Fig. 2, where we show the potential inside one period of a 1D SW in sodium for three values of detuning. Note that  $\Delta$  is taken to be positive so that the potential minimum is at the node of the SW—the atom is then said to be in a “weak-field seeking” state. For comparison, the figure also shows a harmonic potential. Within the SW, the saturation parameter varies as  $p = p_0 \cos^2 kx$ . For each value of detuning, the value of  $p_0$  is adjusted so that the curvature near the bottom of the well (and hence the time period of oscillation) is the same.

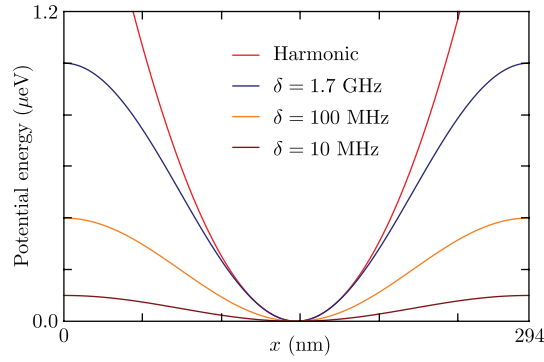


**Figure 2:** Effect of detuning on shape of dipole potential. Potential curves inside one period of a SW for sodium on the  $D_2$  line are shown for three values of detuning: 10 MHz, 100 MHz, and 1.7 GHz. For comparison, the purely harmonic potential is also shown. The intensity for each detuning is adjusted so that the potential has the same curvature near the bottom as the harmonic potential.

### 3 Experimental Details

The experiment consists of using a SW of near-resonant light as an array of lenses to focus sodium atoms as they pass through the light, and allowing the focused atoms to deposit on a silicon substrate where they can be imaged with a scanning tunneling microscope (STM).

The setup is shown schematically in Fig. 3. The sodium source is maintained at 420°C in an ultra-high vacuum (UHV) chamber maintained at a pressure below  $10^{-10}$  torr using an ion pump. The source produces a beam of atoms with an rms velocity of about 860 m/s and a transverse collimation of about 3 mrad (corresponding to a velocity of 2.6 m/s or a temperature of 9 mK) near the SW interaction region. The collimation is further improved using 1D molasses cooling below the SW. The silicon substrate (typically  $6 \times 6$  mm<sup>2</sup>) is clamped rigidly with respect to a mirror used to retroreflect the incoming SW and molasses beams. This ensures that there is no variation in the spatial phase of the SW during deposition. The substrate intersects the SW beam near the intensity maximum and the atoms deposit after the interaction with negligible free flight.

All the laser beams are derived from a Coherent 899-29 ring dye laser operating with Rhodamine-6G dye at 589 nm. The linewidth of the laser is below 1 MHz. Its output is locked to the required hyperfine transition of the sodium  $D_2$  line ( $3S_{1/2} \rightarrow 3P_{3/2}$  transition) in a separate absorption cell using FM Doppler-free spectroscopy. For this transition,  $I_s = 6.29$  mW/cm<sup>2</sup> and  $\Gamma/2\pi =$

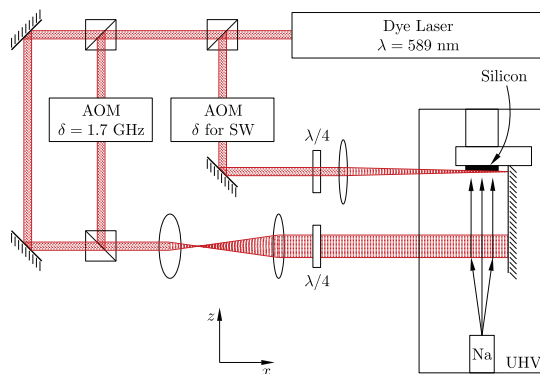


**Figure 3:** Schematic of the experiment.

10 MHz. The required frequency offsets for the SW and molasses beams are produced using acousto-optic modulators (AOMs). Both beams are measured to have approximately Gaussian profiles, with beam waists located at the retro-mirror. The waist radius  $w_0$  is varied for different experiments, as discussed below.

For each deposition, we use a clean silicon sample with a hydrogen passivated surface. The hydrogen is desorbed in UHV by heating the silicon to  $550^\circ\text{C}$ . The *in situ* heating is crucial for obtaining metallic sodium deposition and making good STM imaging contact. The focused atoms form a grating on the silicon surface, which diffracts in the visible spectrum. The diffraction efficiency gives us a reliable estimate of the fidelity of the grating over the sample, which is useful since the STM image only covers an area of  $1\ \mu\text{m}^2$  at a time. The sample is transferred to the STM chamber while in UHV and can be imaged cleanly for a few hours (at  $\leq 10^{-9}$  torr) before surface degradation begins to cause some instability in the scans.

We now consider the details of the focusing process in order to design the optimal atom lens for a thermal atom beam. Most of our studies have used the strongest transition in the sodium  $D_2$  line: from the  $F = 2, m_F = 2$  ground state to the  $F' = 3, m_{F'} = 3$  excited state, coupled using  $\sigma^+$  light. The optical dipole force due to this light within one period of a SW has already been discussed in the last section. In an ideal situation, an atom from a perfectly collimated (i.e. no transverse velocity) and monochromatic (i.e. single longitudinal velocity) beam enters a period of the SW with equal probability across the  $\lambda/2$  potential well. Assuming that the well is perfectly harmonic, the atom has an oscillation period  $T$  independent of its amplitude (entry point in the well). Therefore, after a time  $T/4$ , all the atoms are at the bottom of the well and the beam is perfectly focused.

Within this simple model, we can now understand how the experimental parameters affect the focal width and contrast. First, it is better to have a potential that is as harmonic as possible, which from Fig. 2 means using the largest possible detuning given the total power that we can get from the laser. Large detunings are also advantageous because they give deeper potentials, and atoms are only affected by a potential that is deeper than their initial transverse kinetic energy. Second, in order to be focused by the potential, the atoms must enter the light field in the correct ( $F = 2$ ) ground state. We achieve this in the molasses cooling region. The cooling light (which, as in the SW, drives the  $F = 2 \rightarrow F' = 3$  transition) has mixed into it light exactly resonant with the  $F = 1 \rightarrow F' = 2$  transition, produced using the  $\delta = 1.7$  GHz AOM in the experimental schematic shown in Fig. 3. This serves the dual purpose of pushing the thermal population of  $F = 1$  ground-state atoms into the  $F = 2$  ground state, and preventing optical pumping into the  $F = 1$  ground state during the cooling cycles.

The interaction time in the SW determines how well we satisfy the  $T/4$  timing condition. It depends on the longitudinal velocity of the atoms and the waist diameter of the SW beam. Since we use a thermal beam, we have a range of longitudinal velocities and, for each velocity, the focal point is slightly different. This is analogous to the effect of chromatic aberrations when focusing white light. The effect can be reduced by making  $T$  as small as possible (by making  $w_0$  small), so that variations in matching the  $T/4$  condition are less severe.

The effect of collimation of the atom beam is similar, since it determines the initial transverse velocity with which atoms enter the potential well. With a finite initial velocity, a given atom reaches the bottom of the potential at a time different from  $T/4$ . This has an adverse effect on spot size much as collimation does in ray optics. The effect can again be alleviated by reducing  $T$ , because a smaller  $T$  means that the transverse velocity acquired by the atoms when they reach the bottom of the well is larger and the effect of the initial velocity is less severe.

To summarize, the above analysis indicates that we can obtain narrowly focused lines with good atomic beam collimation; large, positive detunings; and a small interaction length.

## 4 Results and Discussion

The experimental results support the general features of the analysis presented above. In Fig. 4, we

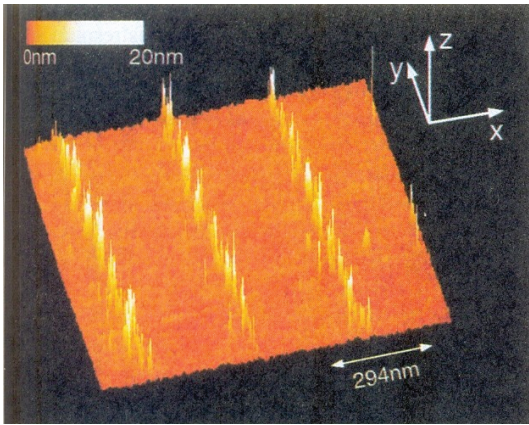


**Figure 4:** STM micrograph of sodium deposited on silicon under optimal focusing conditions. The sodium distribution was obtained from a 35 s deposition under the following conditions in the SW:  $\delta = +1710$  MHz,  $w_o = 56 \mu\text{m}$ , and power of 8 mW in each traveling wave. The molasses beam was set to polarization-gradient cooling with parameters:  $\delta = -12$  MHz,  $w_o = 5$  mm, and power of 50 mW in a lin  $\perp$  lin configuration. The resultant linewidth is about 20 nm and the contrast is about 10:1.

show a STM micrograph of sodium distribution under optimal focusing conditions, as listed in the figure caption. The polarization-gradient cooling used in the molasses results in a transverse temperature of about  $25 \mu\text{K}$ . The SW beam had a confocal parameter of 1.3 cm, which is the smallest we can use given the 5 mm distance from the sample to the mirror. The sodium grain size from this 35 s deposition is about 6 nm near the line center. The full width at half maximum of the line is 20 nm and the interline contrast is about 10:1; in fact, the roughness of the region between the lines is the same as that of a bare silicon surface, indicating that there is very little sodium present. The high contrast we obtain is partly due to good state preparation. With insufficient repumping light in the molasses beam, a significant fraction of the atoms exit the cooling region in the  $F = 1$  ground state, forming a uniform background of unfocused atoms.

The importance of collimation and interaction length is shown in Fig. 5. The detuning and power in the SW were the same as those for Fig. 4. In Figs. 5(a) and 5(b), the beam was collimated using ordinary Doppler molasses cooling, which as discussed before results in a higher transverse temperature (of about  $240 \mu\text{K}$ ), while in Fig. 5(c) the cooling was completely turned off. The roughly linear degradation with both collimation and interaction length is evident from the

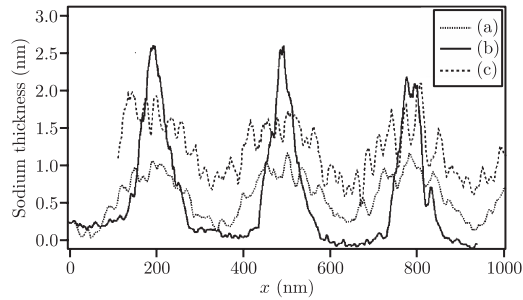
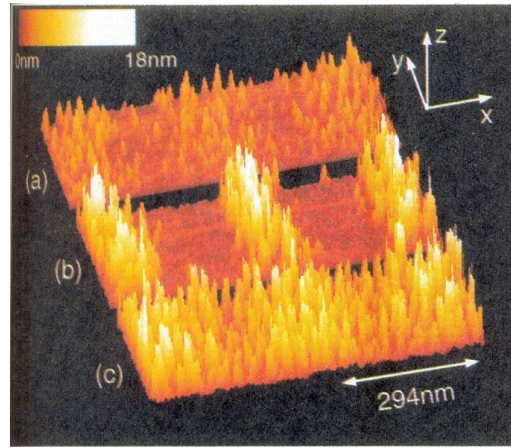


**Figure 5:** Effect of different experimental parameters on sodium focusing. In (a) and (b), the beam was collimated with ordinary Doppler molasses using  $\delta = -5$  MHz,  $w_o = 5$  mm, and an input power of 7.5 mW with  $\sigma^+$  polarization, while in (c) the cooling was turned off completely. In (a) the SW interaction length was increased by a factor of 4 ( $w_o = 224 \mu\text{m}$ ), while in (b) and (c) it was the same as that for Fig. 4 namely  $56 \mu\text{m}$ . The poor focusing in (c) actually required us to run for 50% longer in order to get sufficient image contrast, hence the overall increase in area under the curve. The average line profiles from the three images are shown below.

average line profiles across the three STM images shown in the lower portion of the figure.

The dependence on SW detuning, seen from the line profiles in Fig. 6, is consistent with our expectations from the shape of the potentials in Fig. 2. The focusing conditions are the optimal conditions used for Fig. 4, except for the two detunings. At  $\delta = 100$  MHz, the focusing is poorer with the contrast being noticeably degraded, mainly because of the larger anharmonic content. The depth of the potential at this detuning ( $\sim 4$  mK) is not a factor when the molasses cooling is on. However, it does become significant when the cooling is turned off (which makes the transverse temperature  $\sim 9$  mK): we do

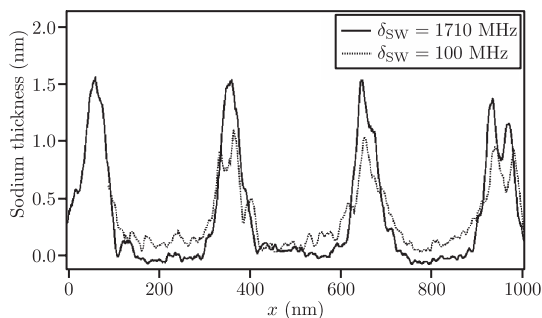


**Figure 6:** Effect of detuning. The line profiles are from images taken under the same SW conditions as that for Fig. 4, except for the input power at  $\delta = 100$  MHz scaled down to  $700 \mu\text{W}$  to match the timing condition.

not observe any focusing under the conditions in Fig. 5(c) when  $\delta = 100$  MHz.

We have also studied the focusing as a function of intensity. We see only a 20% variation in linewidth over a range of a factor of 2. This is partly due to the thermal longitudinal velocity spread, which guarantees that some velocity group meets the  $T/4$  condition over this intensity range. It also indicates that chromatic aberrations are not very important at these focal widths.

## 5 Conclusions

In conclusion, we have reviewed the two kinds of forces that near-resonant light can exert on atoms. We use the spontaneous force to cool and collimate an atomic beam, and the dipole force inside a standing wave to focus the atoms.



**Vasant Natarajan** did his B.Tech. from IIT, Madras; his M.S. from RPI, Troy, NY, USA; and his Ph.D. from MIT, Cambridge, MA, USA. He then worked for two years at AT&T Bell Labs, Murray Hill, NJ, USA. He joined the

Physics Department at IISc in 1996, where he has been ever since. His research interests are in laser cooling and trapping of atoms; quantum optics; optical tweezers; quantum computation in ion traps; and tests of time-reversal symmetry violation in the fundamental laws of physics using laser-cooled atoms.

By studying the shape of the potential, we predict that the optimal focusing conditions require large detunings and a short focal length. These considerations are borne out by the experimental results, and allow us to focus atoms down to a size of 20 nm. This kind of atom lithography is an example of the field of **atom optics**, where light is used to manipulate matter which is a role reversal from ordinary optics where matter is used to manipulate light.

## Acknowledgments

The experimental part of this work was done when I was employed at AT&T Bell Labs during the period 1993–95. I am grateful to my student Ketan Rathod for help with the figures.

Received 5 June 2014.

## References

1. V. Natarajan, R. E. Behringer, and G. Timp, “High-contrast, high-resolution focusing of neutral atoms using light forces,” *Phys. Rev. A* **53**, 4381–4385 (1996).
2. J. Dalibard and C. Cohen-Tannoudji, “Laser cooling below the Doppler limit by polarization gradients: Simple theoretical models,” *J. Opt. Soc. Am. B* **6**, 2023–2045 (1989).
3. P. J. Ungar, D. S. Weiss, E. Riis, and S. Chu, “Optical molasses and multilevel atoms: Theory,” *J. Opt. Soc. Am. B* **6**, 2058–2071 (1989).
4. J. Dalibard and C. Cohen-Tannoudji, “Dressed-atom approach to atomic motion in laser light: The dipole force revisited,” *J. Opt. Soc. Am. B* **2**, 1707–1720 (1985).